ORIGINAL ARTICLE

Tribological mechanisms of nano-cutting fluid minimum quantity lubrication: a comparative performance analysis model

H. Hegab[2,1] · U. Umer[3] · A. Esawi[4] · H. A. Kishawy[1]

Abstract

The nano-fluid system efficiency is mostly governed by the amount, structure, and characteristics of the nano-additives and the mechanism by which the nano-fluids are distributed and sprayed to the tool–workpiece interface zone. The utilization of nano-additive-based cutting fluid demonstrated significant improvement in the wear behavior of the cutting tool. They also provide excellent cooling capabilities when machining is carried out at high temperatures especially when cutting difficult-to-machine workpiece material. The present study offers an in-depth study aided with solid analysis and interpretation for the tribological phenomenon associated with the nano-cutting fluids. In the current study, a relative wear volume model has been proposed and validated for two nano-cutting fluid cases. The presented model reveals that nanotubes offer less induced abrasive wear in comparison with the nanoparticles (i.e., the ratio between the induced nanoparticles wear to the nanotubes wear ranges from 139 up to 360 when the applied forces ranges from 10 up to 3000 N, respectively). To validate the model findings, machining experiments were carried out on Inconel 718 under nano-cutting fluid minimum quantity lubrication (MQL) with different cutting parameters and nano-additive concentrations. Two nano-additives performance have been worked out with the MQL conditions, namely, alumina nanoparticles (Al_2O_3) and multi-walled carbon nanotubes (MWCNTs). The wear on the flank face is determined for each cutting run to evaluate the performance of both nano-cutting fluids. The model estimates found to be consistent with the experimental findings as as MWCNTs showed less tool wear compared with Al_2O_3 (i.e., varied from 2 up to 150% at different cutting speeds and feed rates).

Keywords Nano-cutting fluids · Multi-walled carbon nanotubes (MWCNTs) · Induced nano-additive wear · Al_2O_3 nano-fluid

Nomenclature

a	The contact area radius (case I)
A_{CS}	Interference cross-sectional area of nano-additive with surface
A_N	The nominal area
b	The contact area width (case II)
D_{avg}	Nano-additive average size
E_2	Workpiece Young's modulus
F	The resultant applied force
l	Nanotube length
L	Sliding distance
MQL	Minimum quantity lubrication
MWCNTs	Multi-walled carbon nanotubes
NP	Nanoparticle
NT	Nanotube
N_{NA}	Number of nano-additives
V_{NA}	Wear volume induced by nano-additive
Vol_{NA}	The nano-additive volume
VB	Flank tool wear
wt.%	Nano-additive weight percentage
ρ_{sol}	The resultant nano-fluid density
η_s	The number of nano-additives per nominal area of contact
ϕ	Size distribution of nano-additive
$_{avg}$	Nano-additive size standard deviation
ν_2	Workpiece passion ratio

✉ H. Hegab
Hussien.Hegab@uoit.ca

1 Machining Research Laboratory, Ontario-Tech. University, Oshawa, Ontario L1G0C5, Canada

2 Mechanical Design and Production Engineering, Cairo University, Giza 12613, Egypt

3 Advanced Manufacturing Institute, King Saud University, Riyadh 11451, Saudi Arabia

4 Mechanical Engineering Department, The American University in Cairo, New Cairo 11835, Egypt

1 Introduction

Nowadays, industries in all sectors are in growing need to meet the sustainability requirements. These requirements belong to the triple bottom line (T-B-L) of sustainability. These are mostly based on major environmental concerns with some social and economic needs. These needs originate from the extensive usage of natural resources, harmful environmental impacts, and the current economic challenges. Consequently, implementing the principles of sustainable manufacturing through the current industrial activities became more demanded. Therefore, the scientists have attempted to utilize new sustainable techniques within the cutting processes such as eco-friendly cutting fluids, cooling techniques, and coated and textured cutting tools [1, 2]. Employing environmentally friendly and clean lubrication and cooling techniques became one of the vital requirements. Many environmentally lubrication technologies were proposed such as near dry or minimum quantity lubrication (NDL or MQL), use of cryogenic fluids, as well as dry machining [3, 4]. Furthermore, the application of nano-cutting fluid gives excellent results that show increased tool life and good workpiece quality. They also provide good cooling actions to bear the large amount of heat generation especially when working on difficult-to-machine metals [5, 6]. MQL-nano-fluid based on either nanoparticles or nanotubes showed improved performance with regard to power requirement, surface finish, and tool wear in contrast to the conventional MQL [7, 8]. Despite many past attempts, no clear model is available to clarify and analyze the nano-cutting fluid performance with regard to the qualitative and quantitative tool wear. Thus, the main scope of this work is to integrate the experimental outcomes with proper analysis to reveal the tribological mechanisms for the nano-cutting fluids. In this work, a new analytical model was developed for the tool wear induced by nano-additives. The model is explained and validated for both nanoparticles and nanotube cases. Before presenting the new proposed model, some theoretical concepts are presented in Sect. 2 to physically clarify the role of nano-cutting fluids in machining, as well as the tool wear induced by nano-additives.

2 Nano-cutting fluid mechanisms

Two main MQL-nano-cutting fluid mechanisms are discussed in the open literature: rolling and plowing mechanisms.

The rolling mechanism of MQL-nano-fluid is described as follows [9]:

- The MQL nozzle accelerates the compressed air to utilize its velocity to shear and break the nano-fluid into very fine mist; such process is called atomization.

- This mist could be considered as a thin film of the primary cutting fluid coating the nano-additives. This mist has the ability to penetrate and reach the tool-chip interface zone because of its higher velocity in comparison to the cutting tool, and therefore, it penetrates through the tool pores and grain fractured groves.

- In this way, the cutting tool and workpiece surfaces are occupied by large amount of nano-cutting fluid droplets, and consequently, a tribological film is developed which remarkably enhances the wear behavior and lowers the friction.

- In due course, the concentration of nano-additives increases which in turn increases the density of nano-cutting fluid around the cutting area. Thus, these nanoparticles and nanotubes act as rollers, decreasing the induced friction in the interface zone between the cutting tool and workpiece.

The plowing mechanism of MQL-based nano-cutting fluid is described as follows:

- When the nano-cutting mist is applied in the cutting zone, a large amount of nanoparticles or nanotubes are attached with the workpiece surfaces. Due to the application of high pressure, some nanoparticles are sheared off while others provide a rolling effect [10].

- Because of the high compression along with the incremental increase of the nano-additive loading (i.e., concentration), the shape of the nanoparticles/nanotubes can be changed, boosting shearing behavior. Also, some of these nano-additives are washed away and swept by the fresh nano-fluid stream from the nozzle

- As described [11], the plowed-off nanoparticles/nanotubes leave a fine scaled film on the contact surfaces due to the high pressure. Meanwhile, the nanoparticles that occupied the surface holes were cut off by other nanoparticles. Therefore, higher cutting forces are generated due to that the large amount of nanoparticles in the cutting fluid is trapped inside the workpiece asperities.

- Due to the high normal and shear stresses at the cutting tool-chip interface, the plowed-off nanoparticles/nanotubes leave a fine scaled film. This will result in a fine chemical reaction layer, i.e., a nanoparticle thin film will be developed on the machined surface which provides a shielding effect. This fine film serves as a barrier for heat dissipation into the workpiece. Consequently, high temperatures in the cutting area transform the elasto-hydrodynamic lubrication to the boundary lubrication. An explanatory diagram for the plowing action of nano-additives is shown in Fig. 1.

Due to the high pressure of the wide spread nanoparticles/nanotubes and the gap between the tool-workpiece interface, a high contact resistance is developed
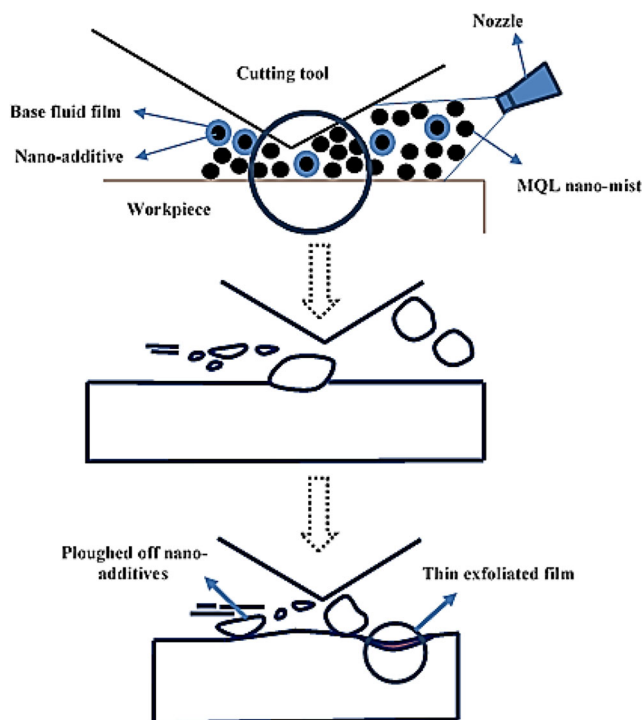
Fig. 1 Plowing mechanism for MQL-nano-cutting fluid [5]

[12], resulting in a very fine nano-additives layer on the workpiece surface as depicted in Fig. 3. Additionally, as the machining proceeds, the increase in amount of nanoparticles/nanotubes assists the growth of the shielding layer on the surfaces of the workpiece.

Equation (1) describes the volume of induced abrasive wear due to nano-additives plowing. It is evident that the volume V_{NA} due to induced abrasive wear is proportional to the interface area between surface and nano-additives (A_{CS}) [13]. In Eq. (1), ø is the nano-additives size distribution, d is the separation distance between the workpiece and cutting tool surface, L is the sliding distance, and $\eta(y)$ is the density of the nanoadditives over the specific contact area.

$$\frac{V_{NA}}{L} = \int_d^\infty n_e(y)\, \text{ø}(y)\, A_{CS}\, dy \tag{1}$$

3 The induced wear model due to nano-additives

A step-wise procedure is detailed below for the comparative wear model due to nano-additives:

Step 1: the ratio of η_{NP} to η_{NT} at same nano-additive distribution, weight percentage, diameter, and separation distance is given by Eq. (2), where D is the size of nano-additives.

$$\frac{n_{NP}}{n_{NT}} = \frac{\rho_{sol-NP}\, \rho_{NT}\, l \int_0^\infty \frac{\pi}{4} D^2\, \text{ø}(D)\, dD}{\rho_{sol-NT}\, \rho_{NP} \int_0^\infty \frac{\pi}{6} D^3\, \text{ø}(D)\, dD} \tag{2}$$

Step 2: A normal Gaussian distribution is assumed as given by Eq. (3).

$$\varnothing(D) = \frac{1}{6_{avg}\sqrt{2\pi}} \exp\left[-0.5\left(\frac{D-D_{avg}}{6_{avg}}\right)^2\right] \tag{3}$$

Step 3: Eq. (2) can be approximated as follows:

$$\frac{\int_0^\infty \pi D^2\, \varnothing(D)\, dD}{\int_0^\infty \pi D^3\, \varnothing(D)\, dD} \approx \frac{1}{D} \tag{4}$$

Step 4: Considering the weight percentage limit up to 6% for nano-additives, the density ratio for the nano-fluid can be approximated to the following:

$$\frac{\rho_{sol-NP}}{\rho_{sol-NT}} \approx 1 \tag{5}$$

Step 5: Using the above results, Eq. (2) can be approximated to the following:

$$\frac{n_{NP}}{n_{NT}} = \frac{3}{2}\left(\frac{\rho_{NT}}{\rho_{NP}}\right)\left(\frac{1}{D}\right)(10^3) \tag{6}$$

where $\frac{\rho_{NT}}{\rho_{NP}}$ is the density ratio of nanotubes to nanoparticles; l and D should be in millimeters.

Step 6: The nanotube and nanoparticle interference cross-sectional areas are illustrated according to Hertz contact theory as shown in Fig. 2. The contact radii for nanoparticles and nanotubes are given by Eqs. (7) and (8):

$$a = \sqrt[3]{\frac{3F\left(\frac{1-\nu_{NP}^2}{E_{NP}} + \frac{1-\nu_2^2}{E_2}\right)}{4\left(\frac{1}{R_{NP}}\right)}} \tag{7}$$

$$= \sqrt[3]{\frac{3F\left(\frac{1-\nu_{NP}^2}{E_{NP}} + \frac{1-\nu_2^2}{E_2}\right)}{4\left(\frac{1}{R_{NP}}\right)}}$$

(because E_{NP} is a large value compared with E_2)

$$b = \sqrt[2]{\frac{4F\left(\frac{1-\nu_{NT}^2}{E_{NT}} + \frac{1-\nu_2^2}{E_2}\right)}{\pi l \left(\frac{1}{R_{NT}}\right)}} = \qquad (8)$$

$$= \sqrt[2]{\frac{4F\left(\frac{1-\nu_{NT}^2}{E_{NT}} + \frac{1-\nu_2^2}{E_2}\right)}{\pi l \left(\frac{1}{R_{NT}}\right)}}$$

(because E_{NT} is a large value compared with E_2)

where R is the nano-additive radius, E_2 is the workpiece elastic modulus, ν_2 is the workpiece Poisson ratio, and F is the applied force.

Step 7: As illustrated in Fig. 2, the ratio of the contact area for case I to case II is estimated by Eq. (9), assuming $R_{NT} = R_{NP}$:

$$\frac{A_{CS-I}}{A_{CS-II}} = \frac{\pi a^2}{2bl} = 1.1481 \; F^{\frac{1}{6}} \frac{D^{\frac{1}{6}}}{l^{\frac{1}{2}}} \left(\frac{1-\nu_2^2}{E_2}\right)^{\frac{1}{6}} \qquad (9)$$

Step 8: The ratio $\left(\frac{n_{NP}A_{CS-NP}}{n_{NT}A_{CS-NT}}\right)$ can be worked out using Eqs. (6) and (9). By taking assumption that the sliding distance (L) is not changing in both scenarios, the ratio could be expressed as follows:

$$\frac{n_{NP} A_{CS-NP}}{n_{NT} A_{CS-NT}} = 1.7221 \; F^{\frac{1}{6}} \frac{\sqrt{l}}{D^{\frac{5}{6}}} \frac{\rho_{NT}}{\rho_{NP}} \left(\frac{1-\nu_2^2}{E_2}\right)^{\frac{1}{6}*} \qquad (10)$$

4 Experimental validation and discussion

To validate the model findings, cutting experiments were done on nickel-based alloy (Inconel 718) using nano-cutting fluid and minimum quantity lubrication (MQL) conditions. The tests were carried out under different process parameters. Two nano-additives were compared for the developed wear models, namely, alumina nanoparticles (Al_2O_3) and multi-walled carbon nanotubes (MWCNTs). The wear on the flank face was measured for each cutting test in order to compare the performance of both employed nano-additives. The turning tests were performed on Inconel 718 using CNC turning center (Hass ST-10 CNC) and standard carbide turning inserts (CNMG 120416MR (ISO)). Regarding the nano-fluid preparation, the MWCNTs with 94% purity, 10–30 μm length, and 20 nm average diameter were used, while the properties of used Al_2O_3 nanoparticles were 20 nm size and 95% purity. The rapeseed vegetable oil (ECOLUBRIC E200) was used as primary cutting fluid for both nanoparticles and nanotubes. Furthermore, ultrasonic device (AQUASONIC-50HT) and magnetic mixer (Hot Plate Stirrer-3073-21) were utilized for dispersion and stability purposes. For the MQL operating conditions, the air-nano-fluid mixture was delivered at an air pressure of 0.5 MPa and nominal oil flow rate of 40 ml/h. The L9 orthogonal array based on Taguchi approach was selected for design of experiments as shown in Table 1. A total of nine machining experiments were performed for each strategy at different cutting speeds (v) in meters per minute, feed values (f) in millimeters per revolution, and weight percentage of the nanoparticles and nanotubes (wt.%). It should be stated
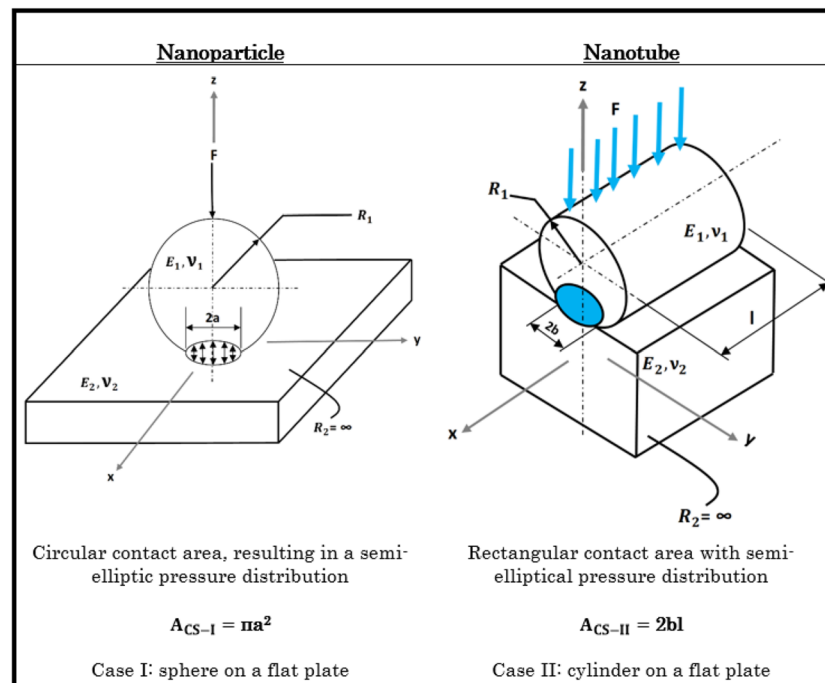

Fig. 2 The contact area schematic for two cases: case I: sphere on a flat plate; case II: cylinder on a flat plate

Table 1 The experimental results for the flank wear

Run no.	V (m/min)	f (mm/rev)	wt.%	VB (mm) for Al$_2$O$_3$-based nano-fluid	VB (mm) for MWCNT-based nano-fluid
1	110	0.09	0	0.45	0.45
2	110	0.14	2.5	0.18	0.165
3	110	0.19	5	0.16	0.158
4	160	0.09	2.5	0.29	0.192
5	160	0.14	5	0.21	0.153
6	160	0.19	0	0.43	0.43
7	210	0.09	5	0.45	0.18
8	210	0.14	0	0.49	0.49
9	210	0.19	2.5	0.42	0.242

that the 9 experiments provided in Table 1 have been conducted one time using Al$_2$O$_3$ and one time for MWCNTs (total of 18 experiments) to facilitate a comparison between the effects of each nano-additive at same feed rate and cutting speed on the measured flank wear. The depth of cut was unchanged for all runs, and it was set as at 0.2 mm. The wear on the flank face of the cutting tool (VB) in millimeters was estimated for each test using tool maker's microscope. A tool-life criterion of 0.4-mm maximum flank wear was selected for all experimental runs.

Table 1 confirms that the application of MQL-based nano-particles and nanotubes cutting fluid systems reduce the wear on the flank face during machining of Inconel 718. It is also obvious that nanotube-based cutting fluid shows better wear behavior than Al$_2$O$_3$ nanoparticle–based cutting fluid at different cutting parameters and concentrations. MWCNTs showed less tool wear compared with Al$_2$O$_3$ (i.e., varied from 2% at cutting test 3 and up to 150% at cutting test 7). As a result of adding nano-additives to the cutting fluid (i.e., when using 2 wt.% or 4 wt.% compared with classical MQL at 0 wt.%), the wetting properties over the flank and rake regions' are enhanced. Therefore, better heat transfer is achieved in comparison to the case of traditional MQL. The improvement in the lubrication conditions as well as the heat dissipation will lead to maintain cutting tool hardness and improvement in tool life. Moreover, the application of nano-additives significantly improves the friction behavior as the applied nano-additives work as rollers in the workpiece-interface zone (see Fig. 1) reducing the sever rubbing and abrasion.

In order to validate the proposed model, the ratio of the wear volume should be worked out for the experimental cases. By incorporating the data shown in Table 2 for Eq. (10), the wear volume ratio can be provided as follows:

$$\frac{V_{NP}}{V_{NT}} = 1083.1 \; F^{\frac{1}{6}} \left(\frac{1-\nu_2^2}{E_2} \right)^{\frac{1}{6}} \tag{11}$$

Inconel 718 is chosen as workpiece material for the validation purpose. The ratio for the wear volume for the workpiece material is given by Eq. (12). Figure 3 shows the effect of resultant force on ratio of wear volume ratio for the selected workpiece material. As illustrated, the induced wear by nano-particles is much higher than that induced by nano-tubes.

$$\frac{V_{NP}}{V_{NT}} = 94.8 \; F^{\frac{1}{6}} \tag{12}$$

The data from Eq. (12) and Fig. 3 indicate that MWCNT-based cutting fluid perform better than Al$_2$O$_3$ nanoparticles fluid with regard to the induced nano-additive wear volume. These findings are in close agreement with the experimental outcomes as provided in Table 1. In addition, another work that has been conducted by the same authors [5] showed micrographs for the tool wear under using MWCNTs, Al$_2$O$_3$, and classical MQL with using the same cutting conditions as can be seen in Fig. 4. The results provided in Fig. 4 confirm the experimental results, and the finding comes from the proposed model as all of them confirm the effectiveness of using MWCNTs over Al$_2$O$_3$ in terms of the tool wear behavior.

To clearly explain these effects, the overall tool wear can be schematically represented in Fig. 5. The overall tool wear is divided into two types: (a) classical tool wear and (b) tool wear because of the induced nano-additive wear. When talking about the classical wear, it means the wear occurred because of the normal cutting motion and the contact between the tool and

Table 2 Nanotubes (MWCNTs) and nanoparticles (Al$_2$O$_3$) size and density

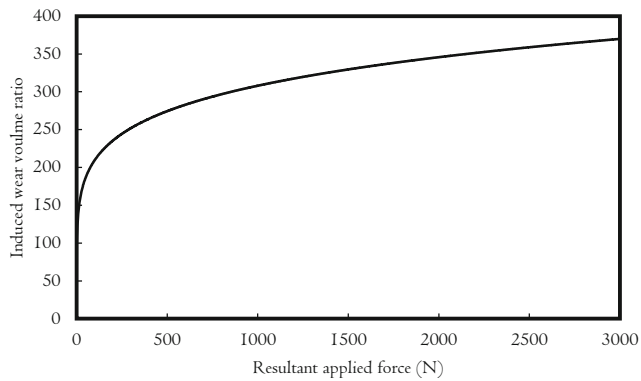|	MWCNTs	Al$_2$O$_3$
ρ (gm/cm^3)	2.1	3.89
D (nm)	20	20
L (nm)	20	--

Fig. 3 The variation in the induced nano-additive wear ratio with the resultant applied force for Inconel 718

workpiece during machining process. The classical flank wear is reduced for both nanotubes and nanoparticles compared with the case where no nano-additives are applied. As discussed earlier, it can be noticed that the application of MQL-nano-fluid under using both nano-additives reduces the severity of this type of wear (classical wear) because of the promising cooling capabilities and reducing the induced friction in the tool-workpiece zone when using nano-additives. Thus, in the illustrated schematic in Fig. 5, it can be found that less classical wear are provided for both types of nano-additives compared with the case without nano-additives.

On the other hand, the plowing effects result in induced nano-additive wear due to the existence of nanoparticles and nanotubes as discussed in Sect. 2. The induced nano-additive wear is the main reason for the second type of tool wear providing in Fig. 5. This type of tool wear can be only noticed when MQL-nano-fluid is applied during machining processes. The results provided in Fig. 3 showed that less nano-additive wear is noticed in case of MWCNTs compared with Al_2O_3 as the ratio between the induced nanoparticles wear to the nano-tubes wear ($\frac{V_{NP}}{V_{NT}}$) ranges from 139 up to 360 when the applied resultant force ranges from 10 up to 3000 N, respectively. Therefore, the tool wear associated with this effect is less in case of MWCNTs. This conclusion is consistent with the

experimental findings as MWCNTs showed less tool wear compared with Al_2O_3 (i.e., varied from 2% at cutting test 3 and up to 150% at cutting test 7). Generally, the proposed model can be satisfactorily used for comparative performance analysis between nanoparticles and nanotubes. The proposed model provides quite correct estimates which are consistent with the experimental findings as both methods (i.e., experimental results and proposed analytical model) show that MWCNTs perform better in comparison to Al_2O_3 nanoparticles.

5 Conclusions and future work

The present study offers an in-depth study aided with solid analysis and interpretation for the tribological phenomenon associated with the nano-cutting fluids. In this work, a relative model for induced wear volume by nanoparticles and nanotubes has been proposed, explained, and validated for both Al_2O_3 and MWCNT-based nano-cutting fluids. To validate the model findings, different machining tests were performed using Inconel 718 as the workpiece material under nano-cutting fluid minimum quantity lubrication (MQL) with different cutting parameters and nano-additive concentrations. Two nano-additives have been used for the MQL-nano-fluid system, namely, alumina nanoparticles (Al_2O_3) and multi-walled carbon nanotubes (MWCNTs). The model estimates are consistent with the experimental findings as MWCNT-based nano-fluid obtains lower values of the flank wear compared with Al_2O_3 nanoparticles. The proposed model can be applied quite satisfactorily for different combinations of nano-fluids and workpiece materials. For future studies, more analytical and experimental investigations will be performed by predicting the induced abrasive wear by nano-additives for different MWCNTs aspect ratios. In this manner, the model will be also able to recommend different parameters of CNTs to be selected.
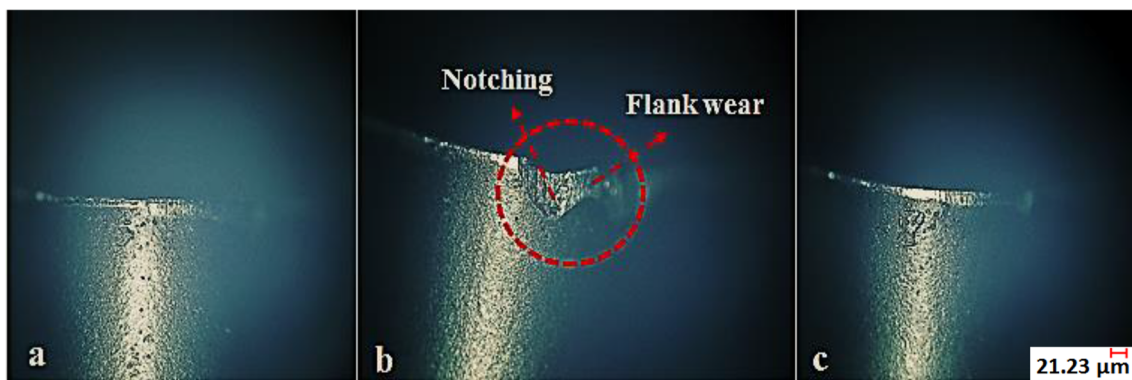

Fig. 4 Typical flank wear observed when using 50 m/min cutting speed and 0.3 mm/rev feed rate (**a**) MWCNTs nano-fluid (**b**) without nano-additives (**c**) Al_2O_3 nano-fluid [5]
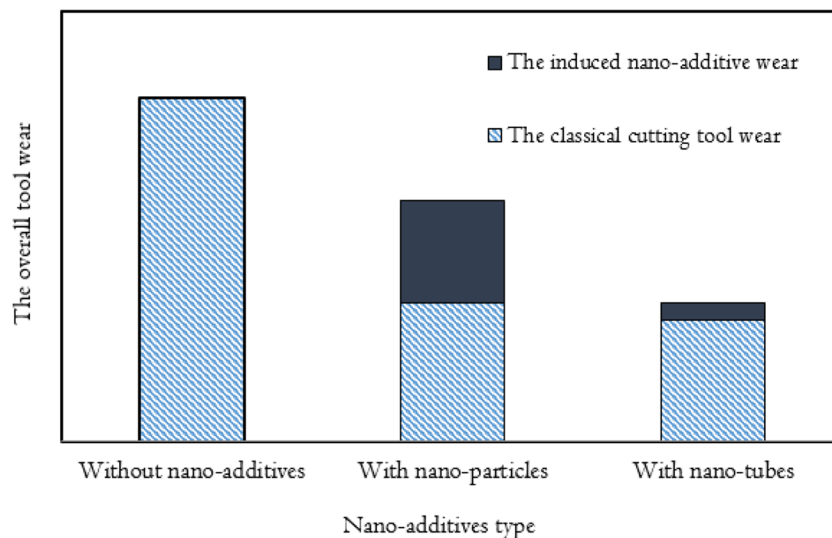
Fig. 5 Total tool wear (classical wear + wear induced by nano-particles) when using nanoparticles, nanotubes and without nano-additives

References

1. Debnath S, Reddy MM, Yi QS (2014) Environmental friendly cutting fluids and cooling techniques in machining: a review. J Clean Prod 83:33–47

2. Ghosh S, Rao PV (2015) Application of sustainable techniques in metal cutting for enhanced machinability: a review. J Clean Prod 100:17–34

3. Klocke F, Eisenblätter G (1997) Dry cutting. CIRP Ann Manuf Technol 46(2):519–526

4. Krolczyk G et al (2017) Dry cutting effect in turning of a duplex stainless steel as a key factor in clean production. J Clean Prod 142: 3343–3354

5. Hegab H, Umer U, Soliman M, Kishawy HA (2018) Effects of nano-cutting fluids on tool performance and chip morphology during machining Inconel 718. Int J Adv Manuf Technol 96(9-12): 3449–3458

6. Hegab H, Umer U, Deiab I, Kishawy H (2018) Performance evaluation of Ti–6Al–4V machining using nano-cutting fluids under minimum quantity lubrication. Int J Adv Manuf Technol 95(9-12):4229–4241

7. Hegab H, Kishawy HA, Gadallah MH, Umer U, Deiab I (2018) On machining of Ti-6Al-4V using multi-walled carbon nanotubes-based nano-fluid under minimum quantity lubrication. Int J Adv Manuf Technol 97(5-8):1593–1603

8. Hegab H, Kishawy H (2018) Towards sustainable machining of Inconel 718 using nano-fluid minimum quantity lubrication. J Manuf Mater Process 2(3):50

9. Mao C, Zhang J, Huang Y, Zou H, Huang X, Zhou Z (2013) Investigation on the effect of nanofluid parameters on MQL grinding. Mater Manuf Process 28(4):436–442

10. Rahmati B, Sarhan AA, Sayuti M (2014) Morphology of surface generated by end milling AL6061-T6 using molybdenum disulfide (MoS 2) nanolubrication in end milling machining. J Clean Prod 66:685–691

11. Rapoport L, Nepomnyashchy O, Lapsker I, Verdyan A, Moshkovich A, Feldman Y, Tenne R (2005) Behavior of fullerene-like WS2 nanoparticles under severe contact conditions. Wear 259(1):703–707

12. Lin Y, So H (2004) Limitations on use of ZDDP as an antiwear additive in boundary lubrication. Tribol Int 37(1):25–33

13. Ghaednia H, Jackson RL (2013) The effect of nanoparticles on the real area of contact, friction, and wear. J Tribol 135(4):041603